On the derivation of the spatial QRS-T angle from Mason-Likar leads I, II, V2 and V5

Daniel Guldenring[1], Dewar D Finlay[1], Raymond R Bond[1], Alan Kennedy[1], James McLaughlin[1], Kieran Moran[2]

[1]University of Ulster, Belfast, United Kingdom
[2]Dublin City University, School of Health & Human Performance, Dublin, Ireland

Abstract

The spatial QRS-T angle (SA) has been identified as a marker for changes in the ventricular depolarization and repolarization sequence. The determination of the SA requires vectorcardiographic (VCG) data. However, VCG data is seldom recorded in monitoring applications. This is mainly due to the fact that the number and location of the electrodes required for recording the Frank VCG complicate the recording of VCG data in monitoring applications. Alternatively, reduced lead systems (RLS) allow for the derivation of the Frank VCG from a reduced number of electrocardiographic (ECG) leads. Derived Frank VCGs provide a practical means for the determination of the SA in monitoring applications. One widely studied RLS that is used in clinical practice is based upon Mason-Likar leads I, II, V2 and V5 (MLRL). The aim of this research was two-fold. First, to develop a linear ECG lead transformation matrix that allows for the derivation of the Frank VCG from the MLRL system. Second, to assess the accuracy of the MLRL derived SA (MSA). We used ECG data recorded from 545 subjects for the development of the linear ECG lead transformation matrix. The accuracy of the MSA was assessed by analyzing the differences between the MSA and the SA using the ECG data of 181 subjects. The differences between the MSA and the SA were quantified as systematic error (mean difference) and random error (span of Bland-Altman 95% limits of agreement). The systematic error between the MSA and the SA was found to be 9.38° [95% confidence interval: 7.03° to 11.74°]. The random error was quantified as 62.97° [95% confidence interval: 56.55° to 70.95°].

1. Introduction

The spatial QRS-T angle (SA) measures the relationship between ventricular depolarization and repolarization. Changes in the depolarization sequence as well as changes in the action potential duration are reflected in the SA [1]. Narrow SA angles indicate a normal relationship between ventricular depolarization and repolarization [2]. A widening of the SA is an indication of an abnormal relationship between ventricular depolarization and repolarization [2]. The properties of the SA have previously been demonstrated to have clinical value in different applications [3, 4]. While the SA has shown to be of clinical value the determination of the SA has proven to be difficult in continuous bedside and ambulatory monitoring applications. This is due to the fact that the determination of the SA requires vectorcardiographic (VCG) data that cannot be easily obtained in monitoring applications. Such VCG data is typically determined by recording the Frank VCG [5] or through derivation from recorded 12-lead ECG data [6]. However, the number and the location of the electrodes that are required for recording the Frank VCG or the 12-lead ECG are not practical in monitoring applications. Derived VCGs that are obtained using monitoring compatible reduced lead systems (RLSs) have the potential of providing a practical means for the determination of the SA in monitoring applications. These RLSs generate the derived VCGs by applying a linear ECG lead transformation matrix to a reduced number of recorded ECG leads. One widely studied RLS that is used in clinical practice is based upon Mason-Likar (ML) [7] leads I, II, V2 and V5 and subsequently refereed to as MLRL system [8]. However, a linear ECG lead transformation matrix that allows for the derivation of the Frank VCG from the MLRL system has not previously been reported in the literature.

The aim of this research is two-fold. First, to develop a linear ECG lead transformation matrix that allows for the derivation of the Frank VCG from the MLRL system. Second, to quantify the errors made when using the MLRL derived SA (MSA) as a substitute for the SA.

2. Material and methods

2.1. Study population

We base our research on a study population of 726

subjects. The study population is composed of normal subjects, subjects with myocardial infarction (MI) and subjects with left ventricular hypertrophy (LVH). One body surface potential map (BSPM) was recorded for each of the 726 subjects in the study population. The study population was randomly partitioned into a training dataset ($DTrain$) and a test dataset ($DTest$). Table 1 details the composition of $DTrain$ and $DTest$.

Table 1. Composition of train data ($DTrain$) and test data ($DTest$).

	Normal	MI	LVH	Total
$DTrain$	172	199	174	545
$DTest$	57	66	58	181

Notes. ***Normal****, Subjects with no abnormalities in their ECGs;* ***MI****, Subjects with myocardial infarction;* ***LVH****, Subjects with left ventricular hypertrophy.*

2.2. BSPM data

The BSPM data used in this research contains electrocardiographic data of 120 leads. One representative QRST complex was calculated for each of the 120 BSPM leads. Three of the 120 leads were recorded from electrodes placed on the right and left wrist and the left ankle (VR, VL and VF respectively). The remaining 117 leads were recorded from thoracic electrodes (81 anterior and 36 posterior recording sites). A comprehensive description of the BSPM data and the recording procedure can be found in [9, 10]. A number of electrocardiographic leads that were required to conduct our research were associated with electrode locations that fell between the locations of the 117 thoracic electrodes. The electrocardiographic data of such leads was obtained using a previously described two-step interpolation procedure [11]. First, the 117 lead BSPMs were transformed into 352 lead BSPMs. This was performed using a Laplacian 3D interpolation method [12]. The location of the 352 thoracic leads corresponded to the nodes in the Dalhousie torso [13]. Second, any required thoracic leads that were located between the 352 thoracic leads were obtained using linear interpolation [14].

2.3. Generation of the Frank VCG

The potentials at the A, C, E, F, H, I and M electrode locations of the Frank lead system [5], were extracted from the BSPMs. The potentials at the Frank electrode locations were used to derive the Frank VCG using (1).

$$\boldsymbol{VCG^{Frank}} = \begin{bmatrix} \boldsymbol{X} \\ \boldsymbol{Y} \\ \boldsymbol{Z} \end{bmatrix} = \boldsymbol{A^{Frank}} \cdot \begin{bmatrix} \boldsymbol{\varphi_A} \\ \vdots \\ \boldsymbol{\varphi_M} \end{bmatrix}. \quad (1)$$

Where $\boldsymbol{\varphi_A}$, $\boldsymbol{\varphi_C}$, $\boldsymbol{\varphi_E}$, $\boldsymbol{\varphi_F}$, $\boldsymbol{\varphi_H}$, $\boldsymbol{\varphi_I}$, and $\boldsymbol{\varphi_M}$ are $1\times N$ vectors that contain N sample values of potentials at the Frank electrode locations A to M respectively, $\boldsymbol{A^{Frank}}$ is a 3×7 matrix of published coefficients [15] that allow for a derivation of the Frank VCG using the potentials $\boldsymbol{\varphi_A}$ to $\boldsymbol{\varphi_M}$, and $\boldsymbol{VCG^{Frank}}$ is a $3\times N$ matrix containing N sample values of the Frank VCG, the $1\times N$ vectors $\boldsymbol{X}$, $\boldsymbol{Y}$ and $\boldsymbol{Z}$ contain N sample values of the three Frank leads X, Y and Z respectively.

2.4. Derivation of the linear ECG lead transformation matrix

The linear ECG lead transformation matrix A^{MLRL}, which allows for the derivation of the Frank VCG from the MLRL system, was derived as follows. First, the Frank VCG leads X, Y and Z of all subjects in $Dtrain$ were concatenated to create the $3\times N$ matrix VCG^{Frank}. Second, the leads I, II, V2 and V5 of all subjects in $Dtrain$, were concatenated to create the $4\times N$ matrix $\boldsymbol{ECG^{MLRL}}$. Third, A^{MLRL} was calculated using least-squares multivariate linear regression as detailed in (2a) and (2b).

$$\boldsymbol{A^{MLRL}} = \\ = \boldsymbol{VCG^{Frank}}(\boldsymbol{ECG^{MLRL}})^{\boldsymbol{T}}[\boldsymbol{ECG^{MLRL}}(\boldsymbol{ECG^{MLRL}})^{\boldsymbol{T}}]^{-1}. \quad (2a)$$

With

$$\boldsymbol{ECG^{MLRL}} = \begin{bmatrix} I \\ II \\ V2 \\ V5 \end{bmatrix}. \quad (2b)$$

Where $[\cdot]^{\boldsymbol{T}}$ and $[\cdot]^{\boldsymbol{-1}}$denote the transpose and the inverse of a matrix respectively, $\boldsymbol{A^{MLRL}}$ refers to a 3×4 matrix of transformation coefficients, $\boldsymbol{VCG^{Frank}}$ is as defined in (1), $\boldsymbol{ECG^{MLRL}}$ is a $4\times N$ matrix of N sample values and $\boldsymbol{I}$, $\boldsymbol{II}$, $\boldsymbol{V2}$ and $\boldsymbol{V5}$ are $1\times N$ vectors that contain N sample values of the MLRL leads I, II, V2 and V5 respectively.

2.5. Generation of the MLRL derived VCG

The four ML leads I, II, V2 and V5 were extracted from the BSPMs and used to derive the Frank VCG through (3).

$$\boldsymbol{VCG^{MLRL}} = \boldsymbol{A^{MLRL}} \cdot \boldsymbol{ECG^{MLRL}}. \quad (3)$$

Where $\boldsymbol{ECG^{MLRL}}$ is as defined in (2b), $\boldsymbol{A^{MLRL}}$ is a 3×4 matrix of transformation coefficients that allow for the derivation of the VCG from the MLRL system and $\boldsymbol{VCG^{MLRL}}$ is a $3\times N$ matrix containing N sample values of the three MLRL derived Frank VCG leads X, Y and Z.

2.6. Determination of the spatial QRS-T angle

The SA and the MSA were calculated as detailed in (4)

to (7).

$$\boldsymbol{QRS_m^d} = \frac{1}{J_p - QRS_{ON}} \sum_{n=QRS_{ON}}^{J_P} \boldsymbol{VCG^d}(n). \quad (4)$$

$$\boldsymbol{T_m^d} = \frac{1}{T_{END} - J_P} \sum_{n=J_P}^{T_{END}} \boldsymbol{VCG^d}(n). \quad (5)$$

$$SA = arccos\left[\frac{\boldsymbol{QRS_m^{Frank}} \cdot \boldsymbol{T_m^{Frank}}}{|\boldsymbol{QRS_m^{Frank}}| \cdot |\boldsymbol{T_m^{Frank}}|}\right]. \quad (6)$$

$$MSA = arccos\left[\frac{\boldsymbol{QRS_m^{MLRL}} \cdot \boldsymbol{T_m^{MLRL}}}{|\boldsymbol{QRS_m^{MLRL}}| \cdot |\boldsymbol{T_m^{MLRL}}|}\right]. \quad (7)$$

Where $\boldsymbol{QRS_m^d}$ is the 3×1 mean vector of ventricular depolarization, $\boldsymbol{T_m^d}$ denotes the 3×1 mean vector of ventricular repolarization, QRS_{ON} is the sample index of the QRS onset, J_P denotes the sample index of the J-point, T_{END} is the sample index associated with the end of the T wave, $\boldsymbol{VCG}^d$ is a $3 \times N$ matrix containing N sample values of the three VCG leads and $d \in \{Frank, MLRL\}$ indicates whether a parameter is derived using the Frank lead system or the MLRL system.

2.7. Performance assessment

The performance assessment was conducted using the differences between MSA and SA. These differences were calculated as detailed in (8).

$$\Delta\boldsymbol{SA} = \boldsymbol{MSA} - \boldsymbol{SA}. \quad (8)$$

Where $\boldsymbol{MSA}$ and $\boldsymbol{SA}$ are vectors that contain the MSA and the SA values of all subjects in $DTest$ and $\Delta\boldsymbol{SA}$ is a vector that contains the differences between the MSA and the SA values of all subjects in $DTest$.

First, the distribution of the elements in $\Delta\boldsymbol{SA}$ was analysed using a histogram. Second, the systematic and the random error component of the differences between MSA and SA were analyzed. The systematic error was quantified as mean [95% confidence intervals (CI)] of the elements in $\Delta\boldsymbol{SA}$. We quantified the random error using the span of the Bland-Altman (BA) 95% limits of agreement [16] as detailed in (9).

$$\text{RandomError} = 2 \cdot 1.96 \cdot std(\Delta\boldsymbol{SA}). \quad (9)$$

Where $std(\cdot)$ denotes the standard deviation and $\Delta\boldsymbol{SA}$ is as defined in (8).

Third, a Breusch-Pagan (BP) test [17] was conducted to assess whether the variance of the differences between MSA and SA is dependent upon the SA value. Forth, the strength of the linear relationship between MSA and SA was quantified using the sample Pearson correlation coefficient.

3. Results

Using multivariate linear regression on the training data the coefficients of the linear ECG lead transformation matrix were found to be:

$$\boldsymbol{A^{MLRL}} = \begin{bmatrix} 0.5953 & -0.3134 & 0.2355 \\ 0.0431 & 0.6536 & -0.0280 \\ -0.0284 & 0.0680 & -0.5095 \\ 0.4157 & 0.0296 & -0.2428 \end{bmatrix}^T.$$

Where $[\cdot]^T$ denotes the transpose of the matrix.

The distributional character of the elements in $\Delta\boldsymbol{SA}$ is depicted in the histogram in Figure 1.

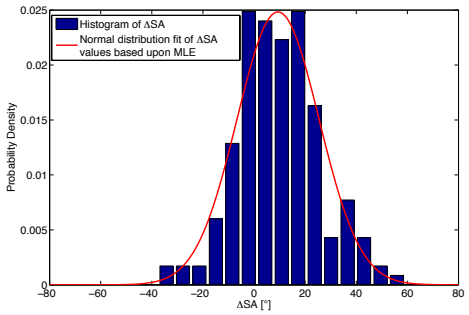

Figure 1. Histogram of the elements in $\Delta\boldsymbol{SA}$ and maximum likelihood normal distribution fit of the $\Delta\boldsymbol{SA}$ values.

It can be seen from Figure 1 that the histogram of the elements in $\Delta\boldsymbol{SA}$ is well described by a maximum likelihood normal distribution fit. The analysis of the elements in $\Delta\boldsymbol{SA}$ found a systematic error of 9.38° [95% CI: 7.03°; 11.74°] and a random error of 62.97° [95% CI: 56.55°; 70.95°]. Both systematic and random error can be seen in the BA plot that is depicted in Figure 2.

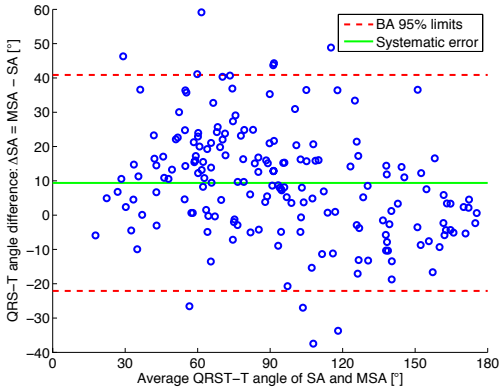

Figure 2. Bland-Altman plot of the differences between MSA and SA over the average angle between MSA and SA.

The distribution of the elements in $\Delta\boldsymbol{SA}$, that is depicted in Figure 2, suggests a constant magnitude of the error variance across the codomain $\{0° \leq SA \leq 180°\}$ of the SA. The linear dependence of the error variance (variance of the difference MSA-SA) from the SA value was formally assessed using the BP test. No evidence $p = 0.82$ for a linear relationship between the error variance and the SA value was found based upon the BP test. This

finding and the distribution of the ΔSA values in Figure 2 indicate that the magnitude of the random error can be considered constant across the entire codomain of the SA. The strength of the relationship between the SA and the MSA was quantified to be 0.928 [95% CI: 0.905; 0.950] using the sample Pearson correlation coefficient.

4. Discussion and Conclusion

This paper reported on the design of the linear ECG lead transformation matrix $\boldsymbol{A}^{MLRL}$ that allows for the derivation of the MSA using the MLRL system.

Our findings indicate a strong linear relationship between the MSA and the SA. Nevertheless, the utilization of the MSA as a substitute for the SA is associated with both a systematic error and a random error, with the random error as the dominating error component. The magnitude of the random error component was not found to dependent upon the SA value. The combination of the herein developed linear ECG lead transformation matrix together with the MLRL system provides a monitoring compatible approach for the determination of the MSA as an estimate of the SA.

Another promising application area of the herein developed ECG lead transformation matrix is in the assessment of cardiac safety of drugs. This is because the developed ECG lead transformation matrix can, in addition to the estimation of the SA, also be used for the estimation of the VCG parameters J-Tpeak, Tpeak-Tend and T-wave loop amplitude. These parameters were previously shown to aid in the differentiation of multi-ion channel drug block [18], which has important implications for drug safety.

Acknowledgements

This work has been supported by the Northern Ireland Connected Health Innovation Centre and the PATHway project funded by the European Commission under the Horizon 2020 Programme (Call H2020-PHC-2014, Grant no. 643491).

References

[1] Aro AL, Huikuri HV, Tikkanen JT, Junttila MJ, Rissanen HA, Reunanen A, et al. QRS-T angle as a predictor of sudden cardiac death in a middle-aged general population. Europace 2012; 14(6):872-876.

[2] Scherptong RW, Henkens IR, Man SC, Le Cessie S, Vliegen HW, Draisma HH, et al. Normal limits of the spatial QRS-T angle and ventricular gradient in 12-lead electrocardiograms of young adults: dependence on sex and heart rate. J Electrocardiol 2008; 41(6):648-655.

[3] Borleffs CJW, Scherptong RWC, Man S, van Welsenes GH, Bax JJ, van Erven L, et al. Predicting ventricular arrhythmias in patients with ischemic heart disease: clinical application of the ECG-derived QRS-T angle. Circ Arrhythm Electrophysiol. 2009; 2(5):548-554.

[4] de Bie MK, Koopman MG, Gaasbeek A, Dekker FW, Maan AC, Swenne CA et al. Incremental prognostic value of an abnormal baseline spatial QRS-T angle in chronic dialysis patients. Europace 2013; 15(2):290-296.

[5] Frank E. An accurate, clinically practical system for spatial vectorcardiography. Circulation 1956; 13(5):737-749.

[6] Guldenring D, Finlay DD, Strauss DG, Galeotti L, Nugent CD, Donnelly MP, Bond RR. Reconstruction of the Frank vectorcardiogram from standard electrocardiographic leads: diagnostic comparison of different methods. Conf Proc IEEE Eng Med Biol Soc 2012; (34): 677-680.

[7] Mason RE, Likar I. A new system of multiple-lead exercise electrocardiography. Am. Heart J. 1966; 71(2): 196-205.

[8] Nelwan SP, Kors JA, Meij SH, Boersma H, Simoons ML. Efficacy of a reduced lead set for pre-hospital triage of thrombolytic strategies. Comp Cardiol 2004; (31):5-8.

[9] Kornreich F, Montague T, Rautaharju P. Identification of first acute Q wave and non-Q wave myocardial infarction by multivariate analysis of body surface potential maps. Circulation 1991; 84(6): 2442-2453.

[10] Montague TJ, Smith ER, Cameron DA, Rautaharju PM, Klassen GA, Felmington CS, et al. Isointegral analysis of body surface maps: surface distribution and temporal variability in normal subjects. Circulation 1981; 63(5): 1166-1172.

[11] Finlay DD, Nugent CD, Nelwan SP, Bond RR, Donnelly MP, Guldenring D. Effects of electrode placement errors in the EASI-derived 12-lead electrocardiogram. J Electrocardiol 2010; 43(6): 606-611.

[12] Oostendorp TF, van Oosterom A, Huiskamp G. Interpolation on a triangulated 3D surface. J Comput Phys 1989; 80(2):331-343.

[13] Horáček BM. Numerical Model of an Inhomogeneous Human Torso. Adv Cardiol 1974; 10:51-57.

[14] Schijvenaars BJA, Kors JA, van Herpen G, Kornreich F, van Bemmel JH. Interpolation of body surface potential maps. J Electrocardiol 1995; 28 Suppl 1: 104-109.

[15] Macfarlane PW. Lead systems. In: Macfarlane PW, van Oosterom A, Pahlm O, Kligfield P, Janse M, Camm J, editors. Comprehensive Electrocardiology. 2nd ed. United Kingdom. London: Springer; 2011; p. 375-426.

[16] Bland JM, Altman DG. Statistical methods for assessing agreement between two methods of clinical measurement. Lancet 1986; 1(8476):307-310.

[17] Breusch TS, Pagan AR. Simple Test for Heteroscedasticity and Random Coefficient Variation. Econometrica 1979; 47(5):1287-1294.

[18] Johannesen L, Vicente J, Mason JW, Sanabria C, Waite-Labott K, Hong M, et al. Differentiating drug-induced multichannel block on the electrocardiogram: randomized study of dofetilide, quinidine, ranolazine, and verapamil. Clin. Pharmacol. Ther. 2014; 96(5): 549-558.

Address for correspondence.

Daniel Guldenring
Room 25B05, School of Engineering, Ulster University,
Shore Road, Newtownabbey, Co. Antrim, BT37 0QB
guldenring-d2@email.ulster.ac.uk